

Facile synthesis and characterization of magnetic $\text{MnFe}_2\text{O}_4/\text{CNT}$ nanocomposites

N. Dehghan-Niarostami · F. Taleshi ·
A. Pahlavan · F. Zabihi · M. Ahmadi Taresi

Received: 25 April 2014 / Accepted: 21 August 2014 / Published online: 17 September 2014
© The Author(s) 2014. This article is published with open access at Springerlink.com

Abstract In this paper, the effects of carbon nanotubes (CNTs) were studied as supports for the synthesis of MnFe_2O_4 nanocomposite. The synthesis of nanocomposite powder $\text{MnFe}_2\text{O}_4/\text{CNTs}$ was performed by direct precipitation method in aqueous solution. The prepared samples were analyzed by X-ray diffraction, scanning electron microscopy and Fourier transform infrared spectroscopy. The results represent the considerable change in the MnFe_2O_4 nanoparticle size and also the morphology of $\text{MnFe}_2\text{O}_4/\text{CNT}$ nanocomposite powder from agglomerative into nanorod in shape.

Keywords Carbon nanotube · Nanoparticles · Nanocomposite · Morphology · Direct precipitation

Introduction

In recent years, there has been wide research in the field of nanostructures, especially magnetic nanoparticles [1–3]. Due to their unique characteristics, magnetic nanoparticles have found a special status in various sciences and multiple applications such as biological materials, medicine and

industry [3–8]. Among magnetic nanoparticles, MnFe_2O_4 nanoparticles have attracted most attention among researchers due to their high saturation, low toxicity, good biocompatibility, strong super magnetic properties, drug delivery, audio filters, magnetic heads and magnetic memories and so on [9–14].

Several parameters such as nanoparticle size, purity, morphology, crystallinity and their distribution are important factors influencing the physical properties of nanoparticles [15–22]. These parameters can be affected by their production methods. Among the different methods such as sol–gel [18], hydrothermal [19, 23], reverse micelle [15] and microwave irradiation [14], direct co-precipitation is the most appropriate method to produce MnFe_2O_4 nanoparticles due to its low cost, easy control of the synthesis conditions and high efficiency [24].

On the other hand, carbon nanotubes have been widely used in various fields because of their unique properties. Due to the high aspect ratio of the carbon nanotubes, they prevent the agglomerating of the particles and increase their applicability considerably [25, 26].

In the present paper, we intend to study the effect of applying carbon nanotube support on size and morphology of MnFe_2O_4 nanoparticles prepared by direct precipitation.

Experimental section

Materials and characterizations

To provide the samples, we used manganese chloride tetrahydrate ($\text{MnCl}_2 \cdot 4\text{H}_2\text{O}$ Merk, purity >99 %), iron nitrate hexahydrate [$\text{Fe}(\text{NO}_3)_2 \cdot 6\text{H}_2\text{O}$, Merk, purity >99 %], ammonium hydroxide solution (NH_4OH , Merck, 25 % of ammonia), carbon nanotubes (CNTs, Neutrino China,

N. Dehghan-Niarostami
Department of Physics, Science and Research Branch, Islamic Azad University, Mazandaran, Iran

F. Taleshi (✉) · M. Ahmadi Taresi
Department of Applied Science, Qaemshahr Branch, Islamic Azad University, POBox 163, Qaemshahr, Iran
e-mail: far.taleshi@gmail.com

A. Pahlavan · F. Zabihi
Department of Physics, Sari Branch, Islamic Azad University, Sari, Iran

20 nm < d < 30 nm, purity >95 %), sulfuric acid (H₂SO₄) and nitric acid (HNO₃).

The crystal structure of prepared samples was investigated by X-ray diffraction (XRD, Philips, Cu (K_α) Spectra, λ = 1.54 Å, Pw 1,800). A scanning electron microscope (SEM, Philips, 15 kV, 60 kx) was used to check the morphology of the MnFe₂O₄/CNT nanocomposites. Fourier transform infrared spectroscopy (FT-IR Spectra, Shimadzu, 8,400 s) was used to study the functional groups on the surface of CNTs. In addition, the sizes of MnFe₂O₄ nanoparticles were determined by Scherrer equation.

Functionalization process of carbon nanotubes

To form strong covalent bonds between atomic ions of Fe³⁺ and Mn²⁺ with carbon nanotubes, the nanotube surface must have functional groups of carboxyl or hydroxyl bonds. To remove carbon contamination, thermal oxidation was carried out for 1.5 h in a horizontal electric furnace at 500 °C under air flow condition (the increasing rate of furnace temperature was 10 °C/min). To functionalize the carbon nanotubes, they were sonicated in 100 cc of acidic solution including a combination of H₂SO₄: HNO₃ (6 M) for 30 min; then the solution was stirred for 3 h in 50 °C. Then, the obtained solution was passed through a filter paper and washed with distilled water until it reached pH = 7. At the end, the prepared samples were dried in an oven at 120 °C.

Synthesis of MnFe₂O₄ nanoparticles

To prepare MnFe₂O₄ nanoparticles, first the required amount of Fe(NO₃)₃·6H₂O and MnCl₂·4H₂O is dissolved in 60 cc distilled water at a ratio of (Fe³⁺)/(Mn²⁺) = 2:1 to achieve the stoichiometry of the spinel ferrite. While stirring the mixed Fe³⁺ and Mn²⁺ ions, 6.5 cc of NH₄OH was overflowed into it. Then the obtained solution was stirred up to 30 min at room temperature. Finally, a brown precipitate was formed at the bottom of the container. Following the completion of the process, the resulting brown precipitate was then washed in distilled water and then dried in an oven at 120 °C for 4 h. Then, the obtained dry powders were calcined in a horizontal electrical furnace at various temperatures of 400, 600 and 800 °C.

Synthesis of MnFe₂O₄ nanoparticles decorating carbon nanotubes

To prepare MnFe₂O₄/CNTs nanocomposite powder, first 0.2 g of functionalized CNTs was poured into 60 cc distilled water and sonicated for 10 min. While stirring the resulting solution, a solution containing the required amount of (Fe³⁺)/(Mn²⁺) = 2:1 was added. For

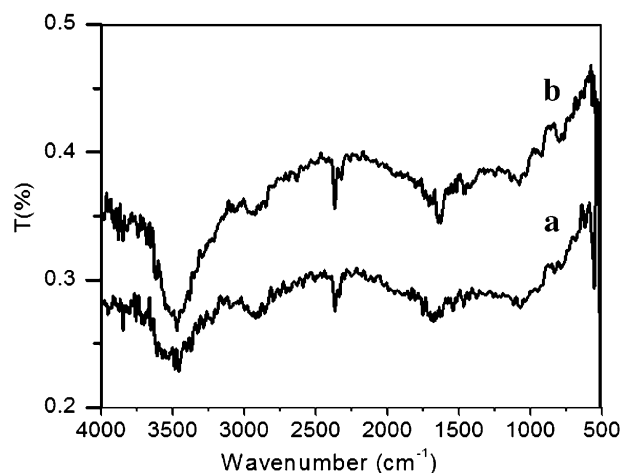


Fig. 1 FT-IR spectrum resulting from CNTs before and after the process of acid treatment

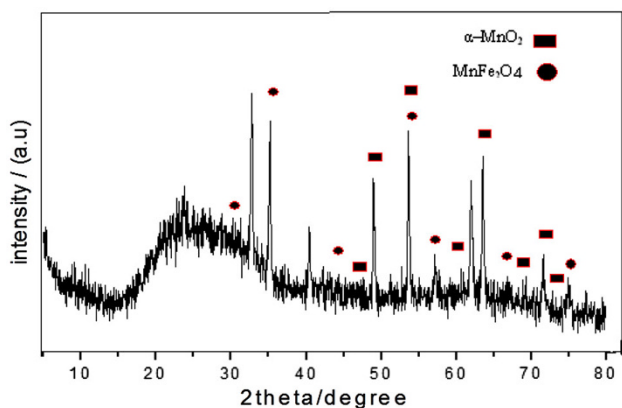


Fig. 2 XRD spectrum for a synthesized sample of MnFe₂O₄ nanoparticles

precipitation, ammonium hydroxide reducer was added instantaneously and the solution was stirred for 30 min. Finally, a dark precipitate was formed at the bottom of the container. Following the completion of the process, it was then washed in distilled water and then dried in an oven at 110 °C for 4 h. Then, the obtained dry powders were calcined in a horizontal electrical furnace at various temperatures of 400, 600 and 800 °C under argon flow condition.

Results and discussion

FT-IR spectrum resulting from CNTs

To study the formation of functional groups on the surface of CNTs, an FT-IR spectrum was prepared. Figure 1 illustrates the FT-IR spectrum resulting from CNTs before

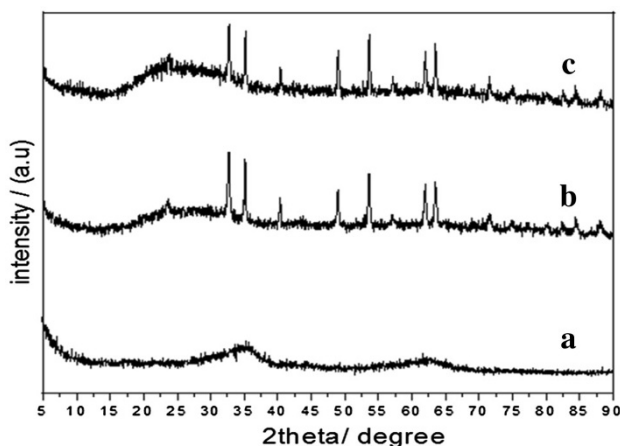


Fig. 3 XRD spectrum for MnFe_2O_4 nanoparticles calcined at: **a** 400 °C, **b** 600 °C and **c** 800 °C

and after the process of acid treatment. Existing peaks in FT-IR spectrum show the formation of functional groups of O–C=O, C–O–O, C–O and C=O, respectively, at wavelengths of 1,210, 1,415, 1,475 and 1,720 (cm^{-1}) [26, 27]. These functional groups play an important role in primary nucleation and formation of MnFe_2O_4 nanoparticles on the surface of carbon nanotubes. $\text{MnFe}_2\text{O}_4/\text{CNT}$ nanocomposite powder is formed through strong chemical bonds between ions of iron atoms and functional groups located on the surface of carbon nanotubes. Due to the high level of carbon nanotubes and large-scale formation of such bonds, they can be applied as an appropriate support for nucleation and better distribution of MnFe_2O_4 nanoparticles on their surface and formation of $\text{MnFe}_2\text{O}_4/\text{CNT}$ s nanocomposite powder.

Analysis of X-ray diffraction spectra

Figure 1 presents the spectra resulting from X-ray diffraction of the prepared samples. Existing peaks in (XRD) spectra within the range of $2\theta = 5\text{--}80^\circ$ suggest the formation of a two-phase structure from MnFe_2O_4 and $\alpha\text{-MnO}_2$ nanoparticles. The peaks in $2\theta = 28.97, 34.06, 43.6, 53.59, 57.21, 64.5$ and 75.2° (shown by circles) are related to MnFe_2O_4 nanoparticles, which are related to the reflection of crystal plates of (220), (311), (400), (422), (511), (440) and (553), respectively [13, 15, 23]. On the other hand, existing peaks located at $2\theta = 47.5, 50.59, 53.59, 60.39, 66.5, 68, 70.52$ and 73.79° (shown by squares) are associated with $\alpha\text{-MnO}_2$ crystal structure which are related to reflection of crystal plates of (510), (411), (440), (531), (002), (202), (541) and (312), respectively [24]. Moreover, the peaks being sharp represent the crystalline order and high crystalline structure of MnFe_2O_4

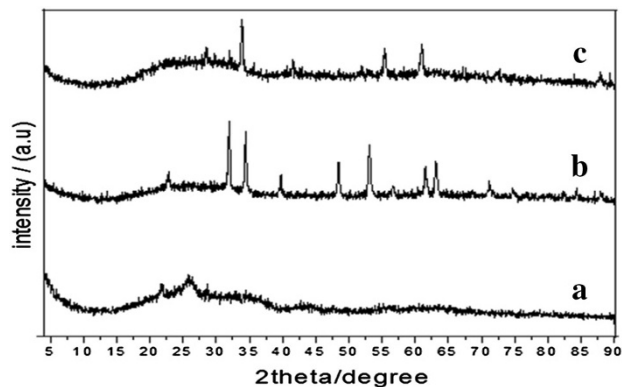


Fig. 4 XRD pattern of $\text{MnFe}_2\text{O}_4/\text{CNT}$ nanocomposite calcined at temperatures of: **a** 400 °C, **b** 600 °C and **c** 800 °C

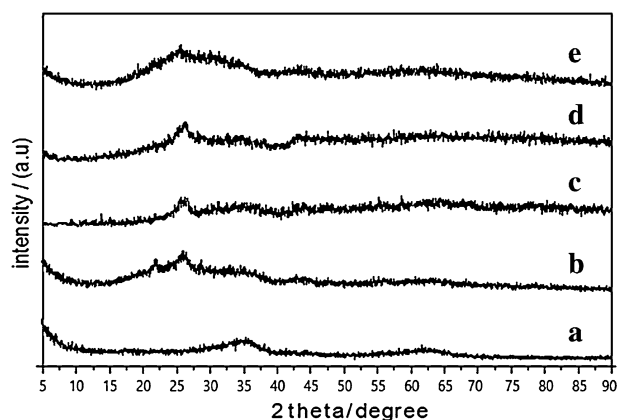


Fig. 5 XRD pattern of $\text{MnFe}_2\text{O}_4/\text{CNT}$ nanocomposite with ratios of: **a** 1:0, **b** 1:1, **c** 1:2, **d** 1:4 and **e** 1:8

nanoparticles. There were no additional peaks, due to the existing impurity in the prepared powder.

An XRD spectrum was prepared to study the effect of calcination temperature on MnFe_2O_4 and $\text{MnFe}_2\text{O}_4/\text{CNT}$ synthesized samples. Figure 3 presents the spectra resulting from XRD of MnFe_2O_4 calcined samples at temperatures of 400, 600 and 800 °C. The average sizes of nanoparticles were determined according to the maximum peak of the XRD spectrum using the Scherrer equation [27]:

$$D = \frac{k\lambda}{\beta \cos \theta} \quad (1)$$

where k is the Scherrer constant (about 0.9), λ is the wavelength of X-ray equal to 1.54 Å, θ is the position of the maximum peak in degrees and β is the full half width at high maximum peak (FWHM) in radians. By Scherrer equation, the size of MnFe_2O_4 nanoparticles was determined to be 3, 60 and 138 nm for samples calcined at

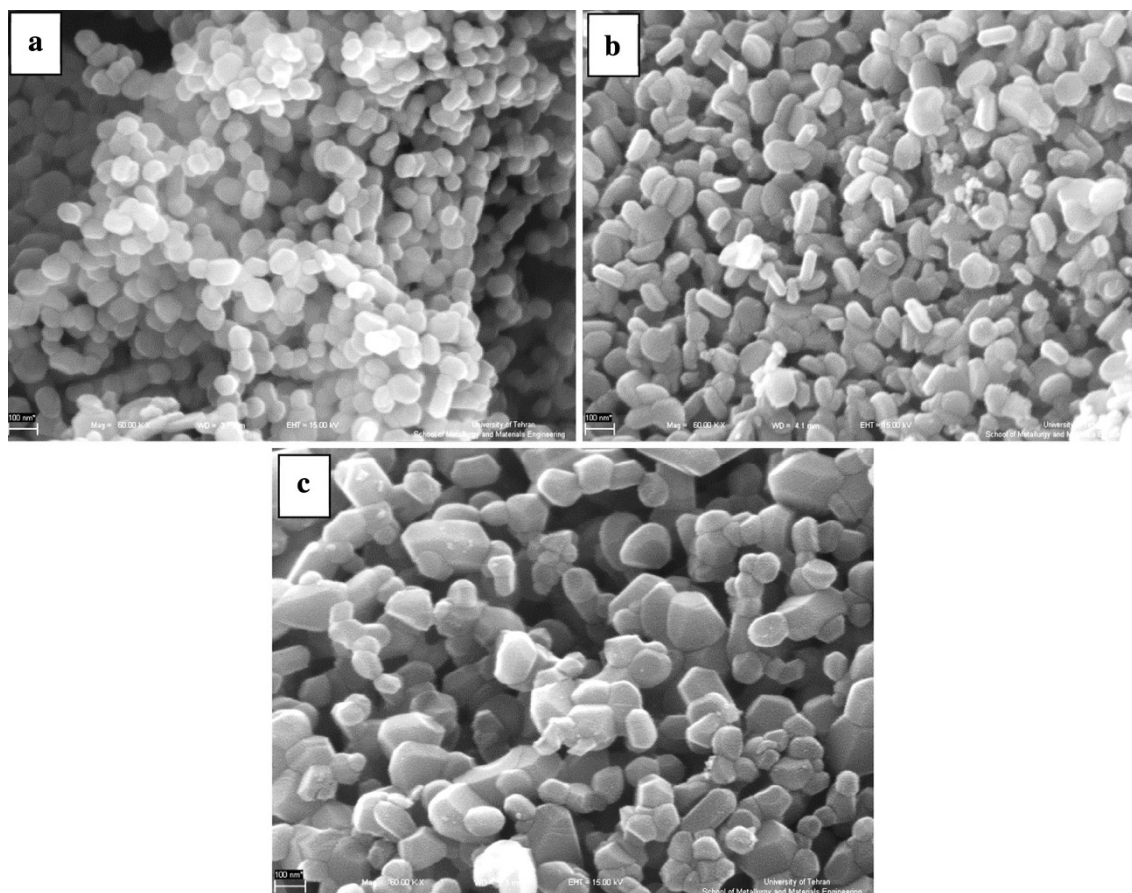


Fig. 6 SEM images of MnFe_2O_4 nanoparticles calcinated at: **a** 400 °C, **b** 600 °C and **c** 800 °C (In all images magnification is $\times 60\text{k}$)

temperatures of 400, 600 and 800 °C, respectively. This result indicates that increasing the calcination temperature will decrease the widths of peaks and increase the size of nanoparticles considerably.

Figure 4 shows the XRD pattern of $\text{MnFe}_2\text{O}_4/\text{CNT}$ nanocomposite powder with a ratio of 1:1 calcined at temperatures of 400, 600 and 800 °C. It was observed that with increase in the calcination temperature, the peaks get sharper and higher. Using Scherrer equation, the average nanoparticle sizes at calcination temperatures of 400, 600 and 800 °C were 11.5, 34.5 and 46 nm, respectively.

After comparing the two XRD spectra in Figs. 3 and 4, for calcined samples at temperature of 400 °C and regarding the result of Scherrer equation, it is observed that the presence of carbon nanotubes' support in the synthesis process increases the mean size of MnFe_2O_4 nanoparticles. The increase in the size of nanoparticles may be due to existing CNTs in solution and the decreased required space for nucleation of MnFe_2O_4 nanoparticles. By increasing the calcination temperature, CNTs prevent the formation of larger crystallite nanoparticles compared to the state of pure MnFe_2O_4 (Fig. 3b, c).

To study the effect of weight ratio of MnFe_2O_4 to CNTs, the composite samples were prepared at a calcination temperature of 400 °C with ratio of 1:1, 1:4 and 1:8 of MnFe_2O_4 to CNTs. The XRD spectrum resulting from the obtained composite powder samples is presented in Fig. 5. According to the XRD spectra, it can be seen that in addition to the associated peaks of MnFe_2O_4 nanoparticles, there is another peak in $2\theta = 26.28^\circ$ estimated to be the (0 0 2) plane of CNTs [26, 27]. On comparing the XRD spectra in Fig. (5b, c), it is observed that by increasing the concentration of CNTs in nanocomposite, the intensity of the related peaks to MnFe_2O_4 will reduce and their widths may increase. Therefore, the size of reduced nanoparticles and their values for ratios of 1:1, 1:2, 1:4 and 1:8 were, respectively, determined to be 11.5, 10.6, 8.9 and 2.3 nm. The decreased size of nanoparticles is due to reduced ionic concentration in solution, increased surface of CNTs and also increased required places for nanoparticles' nucleation.

Figure 6 shows the SEM images of calcinated MnFe_2O_4 nanoparticles at temperatures of 400, 600 and 800 °C. As shown in Fig. 6a for calcinated MnFe_2O_4 nanoparticles at

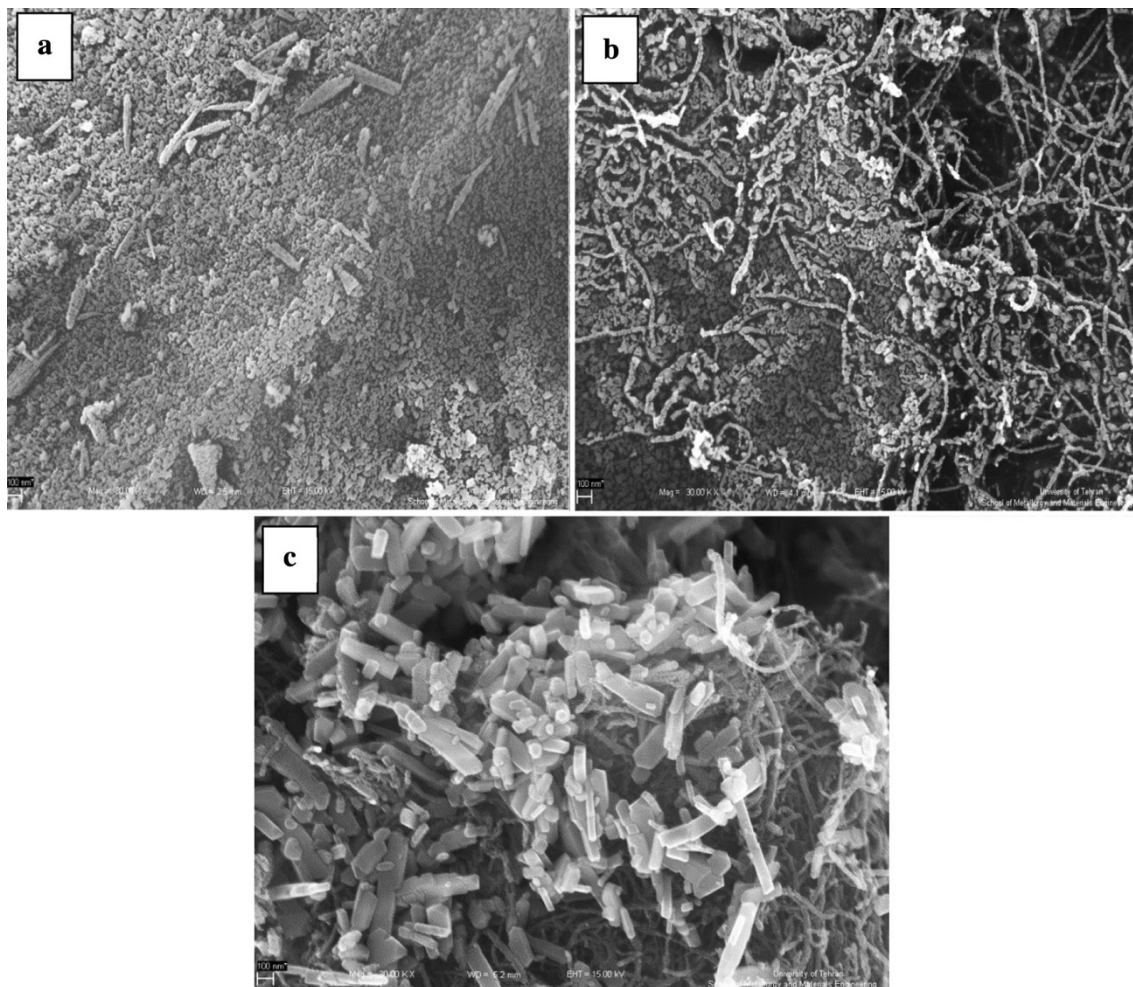


Fig. 7 SEM images of $\text{MnFe}_2\text{O}_4/\text{CNT}$ nanocomposite calcinated at: **a** 400 °C, **b** 600 °C and **c** 800 °C (In all images magnification is $\times 60\text{k}$)

400 °C, nanocrystallites of MnFe_2O_4 with average size of 3 nm are aggregated together to form larger crystallite with a relative size of 77 nm. On increasing the calcination temperature between 600 and 800 °C (Fig. 6b, c), the aggregated particles are increased with an average value of 100 and 141 nm, respectively. The increased size of the particles is due to smaller crystallites sticking together. On the other hand, the geometric shape of crystallites changed from spherical to oval, due to sticking together of two spherical crystallites to form a longer structure.

To study the effect of carbon nanotubes as a support at different calcination temperatures on the morphology of synthesized $\text{MnFe}_2\text{O}_4/\text{CNT}$ nanocomposite powders, SEM images were prepared. Figure 7 shows the SEM images from calcinated $\text{MnFe}_2\text{O}_4/\text{CNTs}$ nanocomposite samples (with 1:1 ratio) at temperatures of 400, 600 and 800 °C. At 400 and 600 °C (Fig. 7a, b), crystallites have stuck together and formed irregular particles among the nanotubes. With increase in the calcination temperature to 800 °C (Fig. 7c), it is observe that in addition to the formation of

ordered strings from $\text{MnFe}_2\text{O}_4/\text{CNTs}$ nanocomposite powder, some crystallites together form cubic-shaped structures. Therefore, increase in the calcination temperature causes the smaller aggregated nanoparticles to permeate into each other and form bigger particles [28].

Conclusion

In this study, MnFe_2O_4 nanoparticles and $\text{MnFe}_2\text{O}_4/\text{CNTs}$ nanocomposite powder were prepared using the direct precipitation method. Noticeable results were obtained in terms of MnFe_2O_4 nanoparticle size. SEM images suggest that nanotubes as nanoparticles growth support will reduce the agglomerated level of nanoparticles and change the powder morphology from the mass state to the string state.

Open Access This article is distributed under the terms of the Creative Commons Attribution License which permits any use, distribution, and reproduction in any medium, provided the original author(s) and the source are credited.

References

1. Yuan, Z., Zhang, L.: *J. Mater. Chem.* **11**, 1265–1268 (2001)
2. Rana, S., Misra, R.D.K.: *JOM.* **57**, 65–69 (2005)
3. Viswanathan, B., Murthy, V.R.K.: *Ferrite Materials, Science and Technology*, p. 198 (1990)
4. Grancharov, S.G., Zeng, H., Sun, S.H., Wang, S.X., O'Brien, S., Murray, C.B., Kirtley, J.R., Held, G.A.: *J. Phys. Chem. B.* **109**, 13030–13035 (2005)
5. Laurent, S., Forge, D., Port, M., Roch, A., Robic, C., Elst, L.V., Muller, R.N.: *Chem. Rev.* **108**, 2064–2110 (2008)
6. Li, X., Hou, Y., Zhao, Q., Wang, L.: *J. Colloid. Interf. Sci.* **358**, 102–108 (2011)
7. Li, S., Lin, Y., Zhang, B., Nan, C., Wang, Y.: *J. Appl. Phys.* **105**, 056105/1–056105/3 (2009)
8. Qiao, R.R., Yang, C.H., Gao, M.Y.: *J. Mater. Chem.* **19**, 6274–6293 (2009)
9. Han, Z., Li, D., Liu, X.G., Geng, D.Y., Li, J., Zhang, Z.D.: *J. Phys. D-Appl. Phys.* **42**, 055008–055012 (2009)
10. Balaji, G., Gajbhiye, N., Wilde, G., Weissmüller, J.: *J. Magn. Magn. Mater.* **242–245**, 617–620 (2002)
11. Lahiri, P., Sengupta, K.: *J. Chem. Soc. Faraday. Trans.* **91**, 3489–3494 (1995)
12. Simsa, Z.: *Phys. Status. Solidi. B.* **96**, 581–587 (1979)
13. Zhao, L., Li, X., Zhao, Q., Qu, Z., Yuan, D., Liu, S., Hu, X., Chen, G.: *J. Hazard. Mater.* **184**, 704–709 (2010)
14. Dom, R., Subasri, R., Radha, K., Borse, P.H.: *Solid. State. Commun.* **151**, 470–473 (2011)
15. Liu, C., Zou, B.S., Rondinone, A.J., Zhang, Z.J.: *J. Phys. Chem. B.* **104**, 1141–1145 (2000)
16. Yang, Y., Jiang, Y., Wang, Y., Sun, Y., Liu, L., Zhang, J.: *Mater. Chem. Phys.* **105**, 154–156 (2007)
17. Hatanaka, S., Matsushita, N., Abe, M., Nishimura, K., Hasegawa, M., Handa, H.: *J. Appl. Phys.* **93**, 7569–7570 (2003)
18. Silva, J.B., Diniz, C.F., Lago, R.M., Mohallem, N.D.S.: *J. Non-Cryst. Solids.* **348**, 201–204 (2004)
19. Sreekumar, K., Sugunan, S.: *J. Mol. Catal. A: Chem.* **185**, 259–268 (2002)
20. Pardeshi, S.K., Pawar, R.Y.: *Mater. Res. Bull.* **45**, 609–615 (2010)
21. Tsoncheva, T., Manova, E., Velinov, N., Paneva, D., Popova, M., Kunev, B., Tenchev, K., Mitov, I.: *Catal. Commun.* **12**, 105–109 (2010)
22. Hou, X., Feng, J., Ren, Y., Fan, Z., Zhang, M.: *Colloids. Surf. A.* **363**, 1–7 (2010)
23. Bujoreanu, V.M., Diamandescu, L., Brezeanu, M.: *Mater. Lett.* **46**, 169–174 (2000)
24. Chen, C., Liang, Y., Zhang, W.: *J. Alloy. Comp.* **501**, 168–172 (2010)
25. Taleshi, F., Hosseini, A.A.: *J. Nanostruc. Chem.* **3**, 356 (2012). doi:[10.1186/2193-8865-3-4](https://doi.org/10.1186/2193-8865-3-4)
26. Ramin, M., Taleshi, F.: *Inter. Nano. Letter.* **3** doi:[10.1186/2228-5326-3-32](https://doi.org/10.1186/2228-5326-3-32) (2013)
27. Venkateswarlu, K., Chandra Bose, A., Rameshbabu, N.: *Phys. B.* **405**, 4256–4261 (2010)
28. Taleshi, F., Pahlavan, A.: *J. Mater. Sci. Mater. Electron.* **25**, 2450–2455 (2014)